The peculiarities of formation of implanted atom concentration beyond the ion range

V.I. Sugakov

Institute for Nuclear Research,
Kyiv, Ukraine

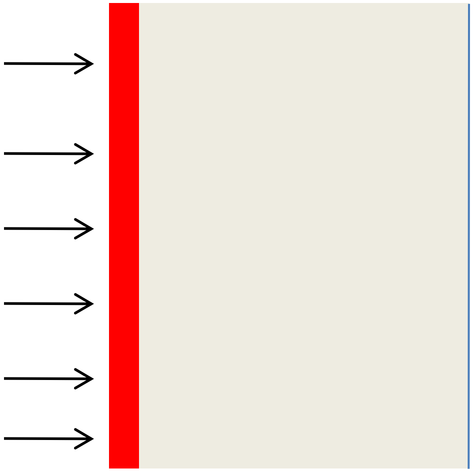

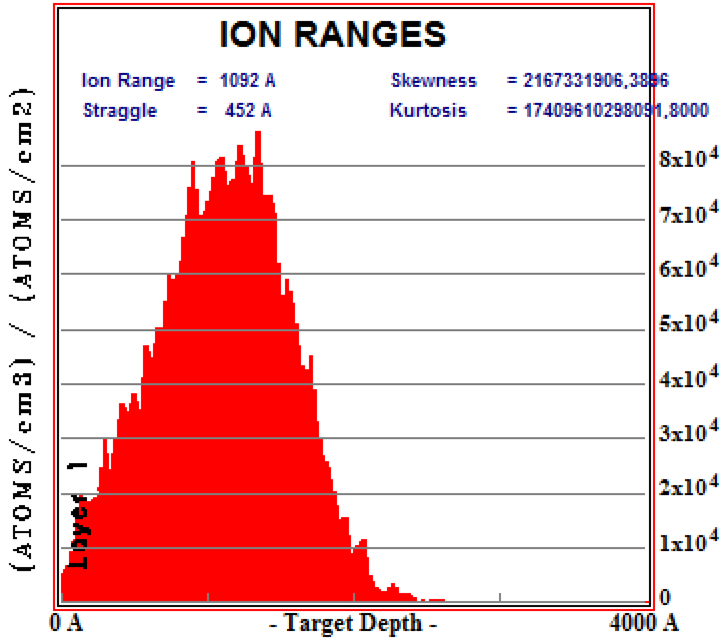

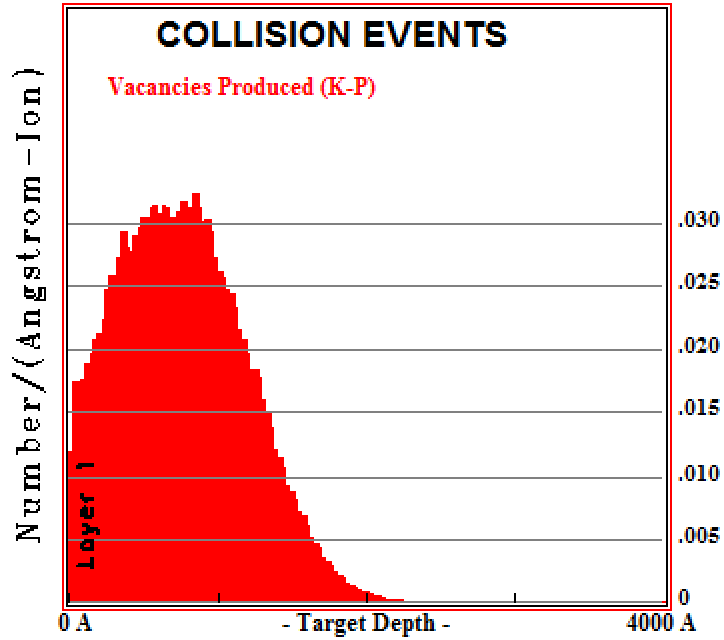

Range

Defects

He in Si, 10 keV

$$E \sim (10 \div 100) keV$$

$$z_p \sim (0.01 \div 0.1) \mu m$$

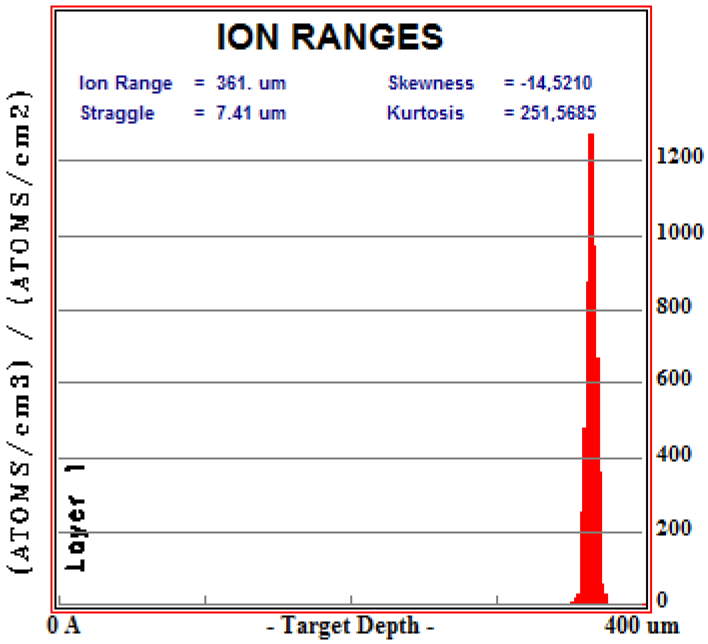

Range

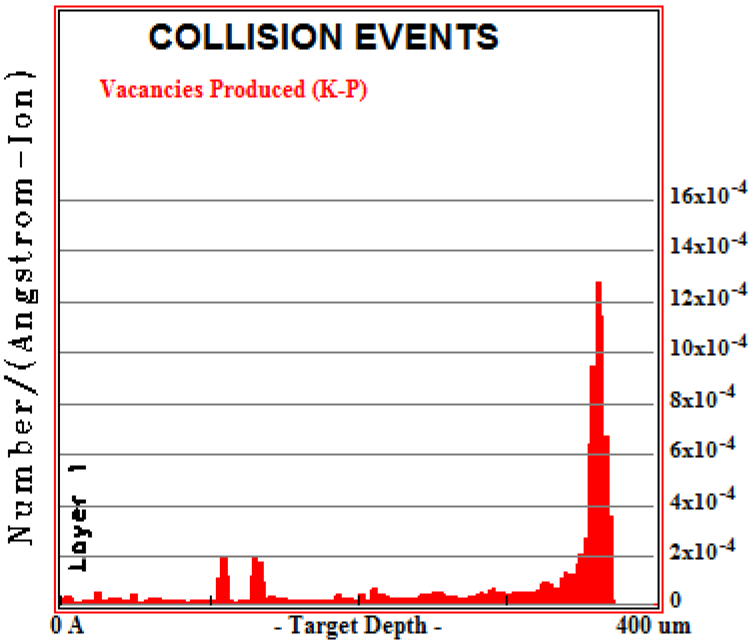

Defects

He in Si, 27 MeV

Long-range effects

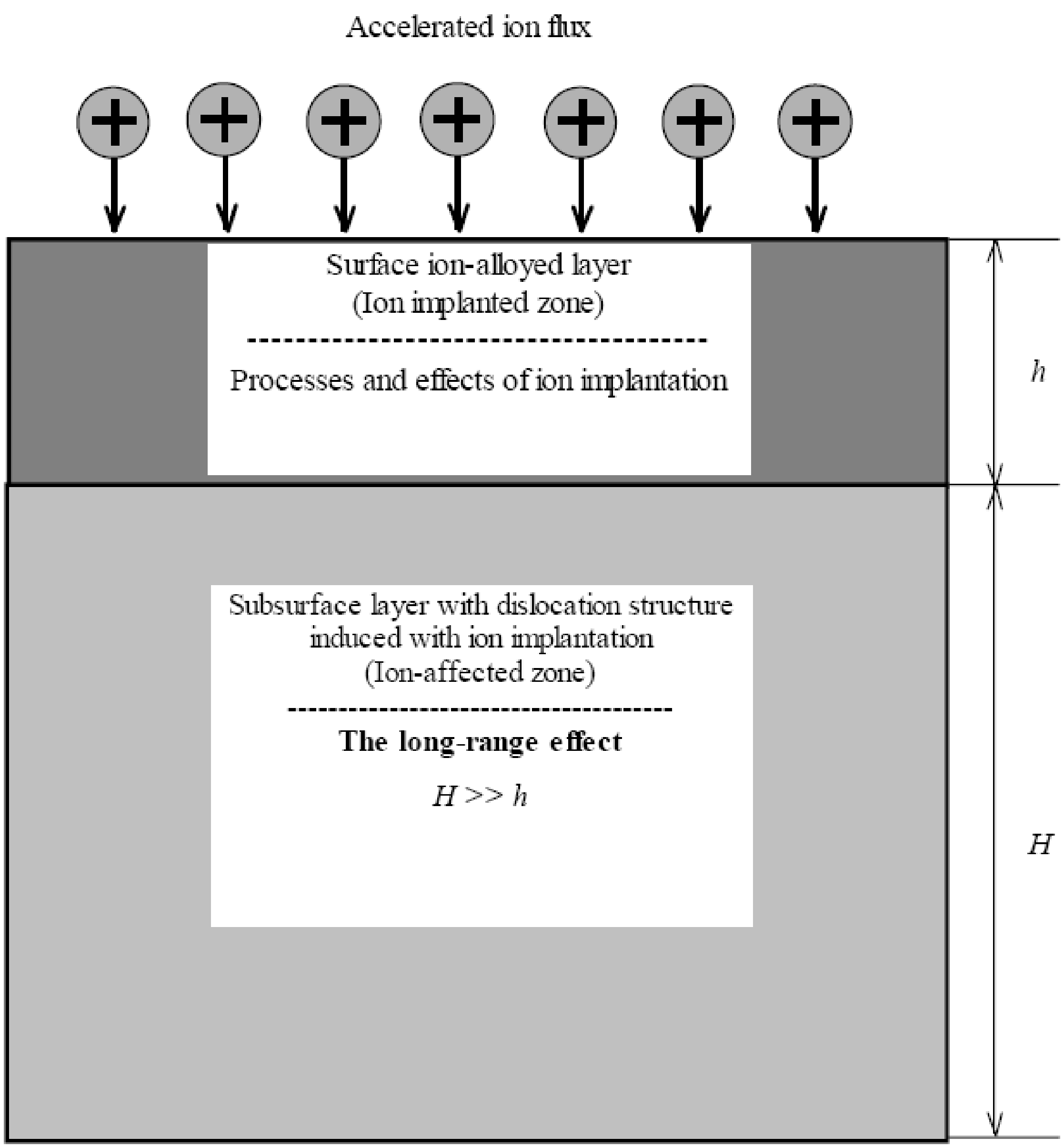

The long-range effect in metal materials at ion implantation

Some effects observed at distances from the surface, which exceed the ion range by several orders of magnitude:

1) the increased microhardness,
2) formation of defects, dislocation structures, voids,
3) phase transitions,
4) the change of the lattice period,
5) an appearance of additional defect layer far from the surface

Models, that were suggested for explanation by different authors

1. Radiation stimulated diffusion.
2. Diffusion in the fields of deformation created by irradiation
3. Shift of dislocations in the fields of deformation
4. Influence of shock waves created by cascades
5. Formation of solitons in multiphase mediums

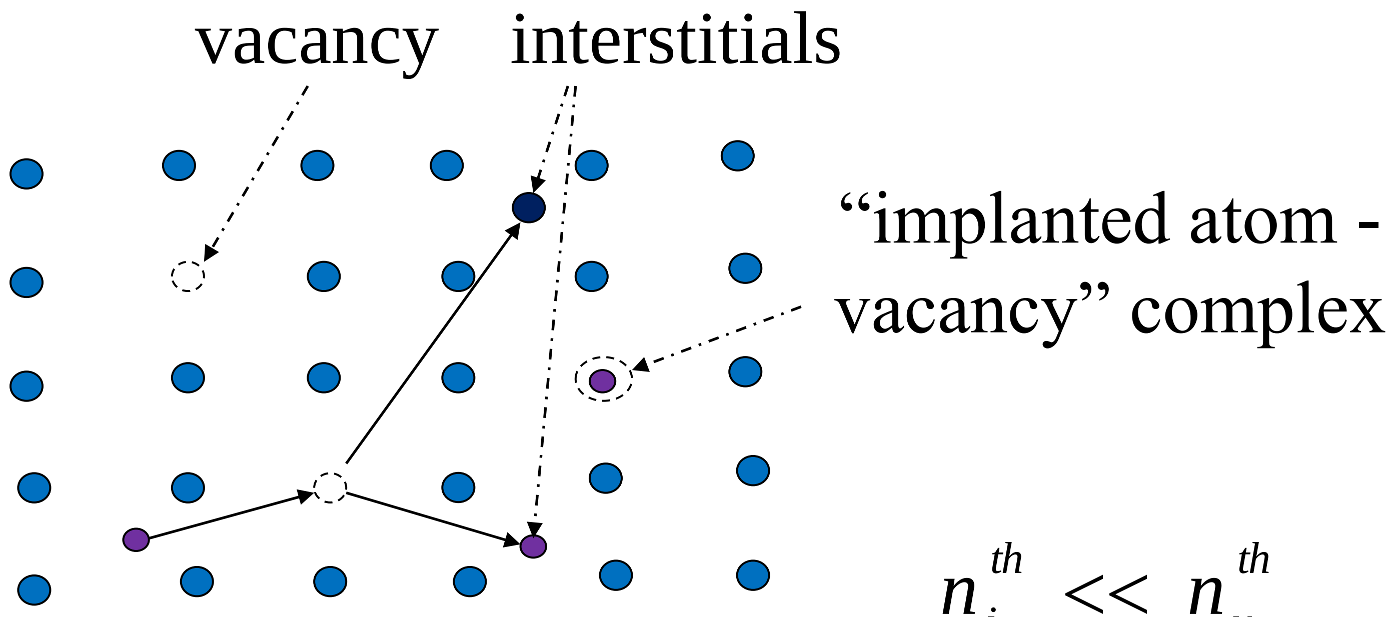

$$n_i^{th} << n_v^{th}$$

The suggested model takes into account the following factors.

1) The total number of the irradiation induced interstitials (intrinsic atoms and implanted atoms) exceeds the number of the vacancies created by the irradiation.

2) There exist immobile complexes of implanted atoms with vacancies.

3) The thermal equilibrium vacancies play an important role in the formation of the properties of the crystal beyond the range.

V.I. Sugakov, Nuclear Physics and Atomic Energy **10**, 395 (2009), Physics of the Solid State **53**, 2131 (2011).

Qualitative picture of the effects

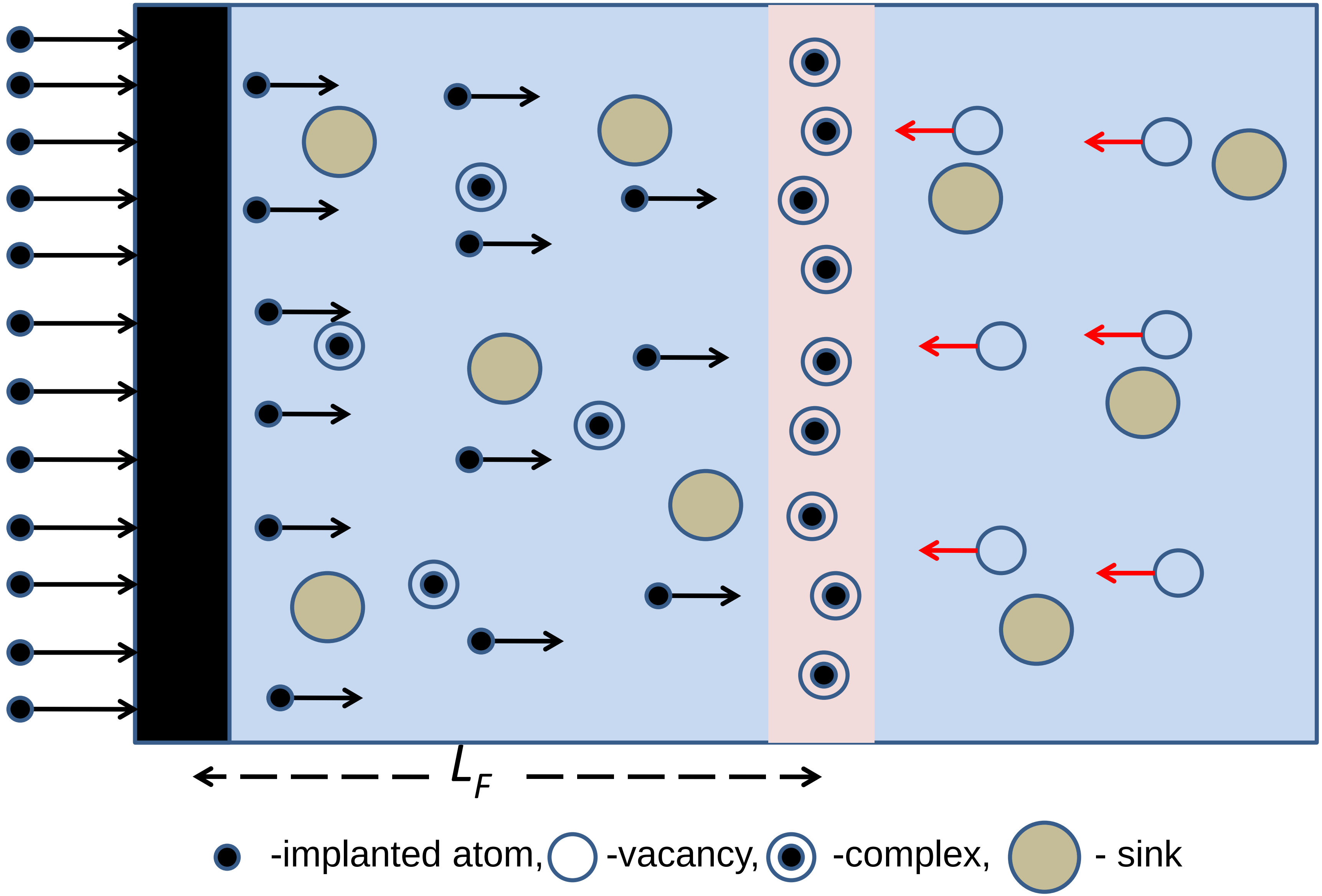

Equations

$$\frac{\partial n_v}{\partial t} = K_v(z) + D_v \frac{\partial^2 n_v}{\partial z^2} - W_{vi} n_i n_v - W_{vp}(n_p n_v - \nu_{pv}^k n_k) - w_{vd}(n_v - n_v^{th})$$

$$\frac{\partial n_i}{\partial t} = K_i(z) + D_i \frac{\partial^2 n_i}{\partial z^2} - W_{vi} n_i n_v - w_{id} n_i$$

$$\frac{\partial n_p}{\partial t} = K_p(z) + D_p \frac{\partial^2 n_p}{\partial z^2} - W_{vp}(n_p n_v - \nu_{pv}^k n_k) - w_{pd} n_p$$

$$\frac{\partial n_k}{\partial t} = W_{vp}(n_p n_v - \nu_{pv}^k n_k)$$

$$K_p(z) = I_p \left(\frac{1}{2\pi}\right)^{1/2} \frac{1}{l} \exp\left(-\frac{(z - z_p)^2}{2l^2}\right) \qquad K_{i(v)}(z) = q_{i(v)} K_p(z)$$

$n_i^{th} << n_v^{th}$

Parameters

$$W_{pv} = 4\pi r_{pv}(D_p + D_v), \qquad D_{v(p)} = D_{ov(op)} Exp(-E_{v(p)} / \kappa T)$$

$$w_{p(i,v)d} = w_{p(i,v)}^{disl} = Z_{p(i,v)}^{disl} \rho_d D_{p(i,v)} \qquad Z_{p(i,v)}^{disl} = 2\pi / \ln \frac{R_d}{r_{p(i,v)d}}$$

$$a = 3 \cdot 10^{-8} cm, \; , \; D_{0v} = D_{0p} = (0.01 - 0.1) cm^2 / s, \quad n_v^{th} = v_o^{-1} \exp(-E_Q / \kappa T)$$

$$R_{pv} = 3a, 5a, 10a \qquad R_{pd} = R_{vd} = 1 / \sqrt{\rho_d}, \; r_{pd} = r_{vd} = a$$

$$E_v = 1.2\, eV, \; E_p = E_i = 0.1\, eV, \qquad E_Q = 1.0\, eV$$

Initial and boundary conditions

$$n_p(0,t) = 0, \; n_i(0,t) = 0, n_v(0,t) = n_v^{th} \qquad n_p(0,t) = 0, \; n_i(0,t) = 0, \; n_v(0,t) = n_v^{th}$$

$$n_p(\infty, 0) = 0, \; n_i(\infty, 0) = 0, n_v(\infty, 0) = n_v^{th}$$

The spatial vacancy distribution at different times (different doses of irradiation)

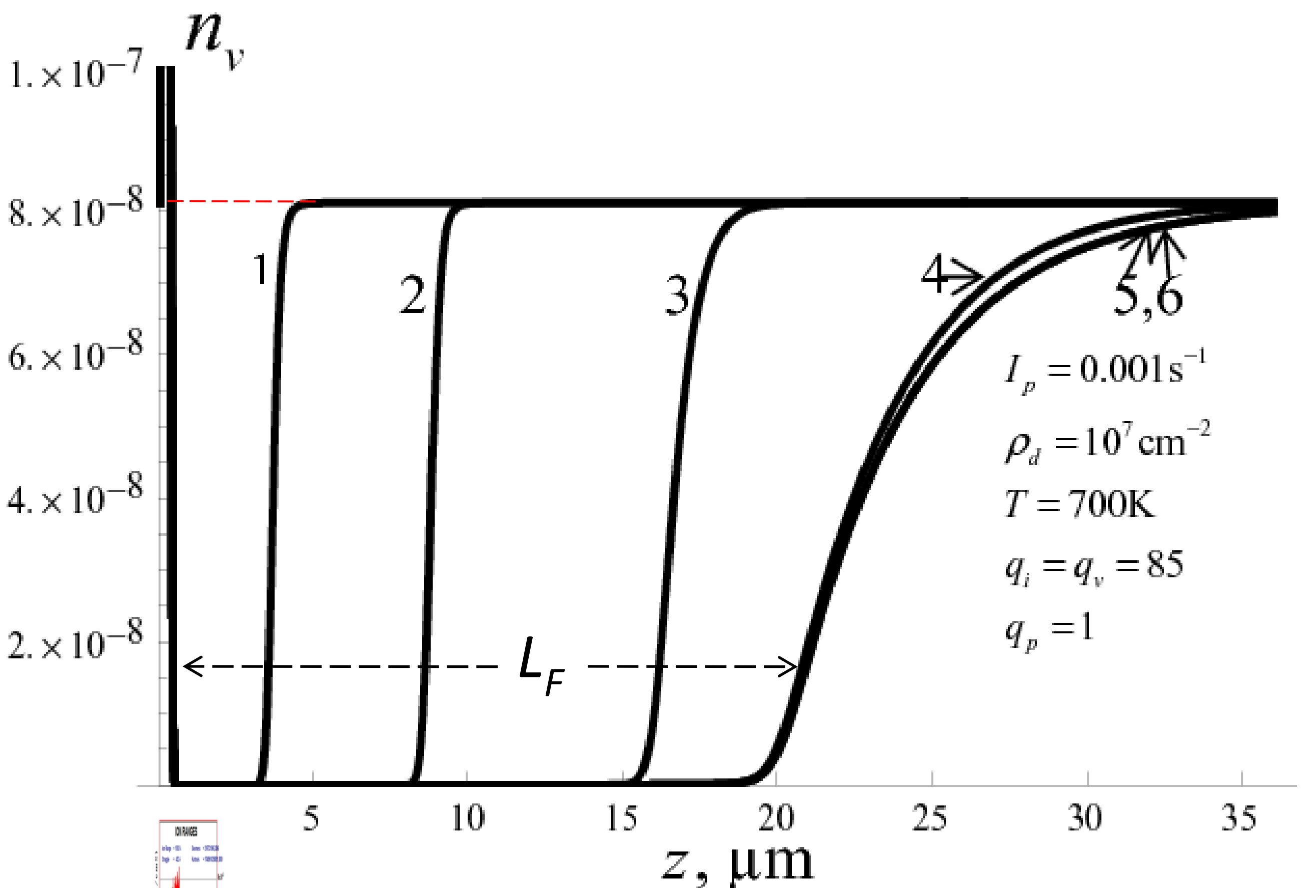

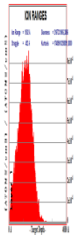

1-10s
2-10^2s
3-10^3s
4-10^4s
5-10^5s
6-10^6s

------- equilibrium vacancy distribution

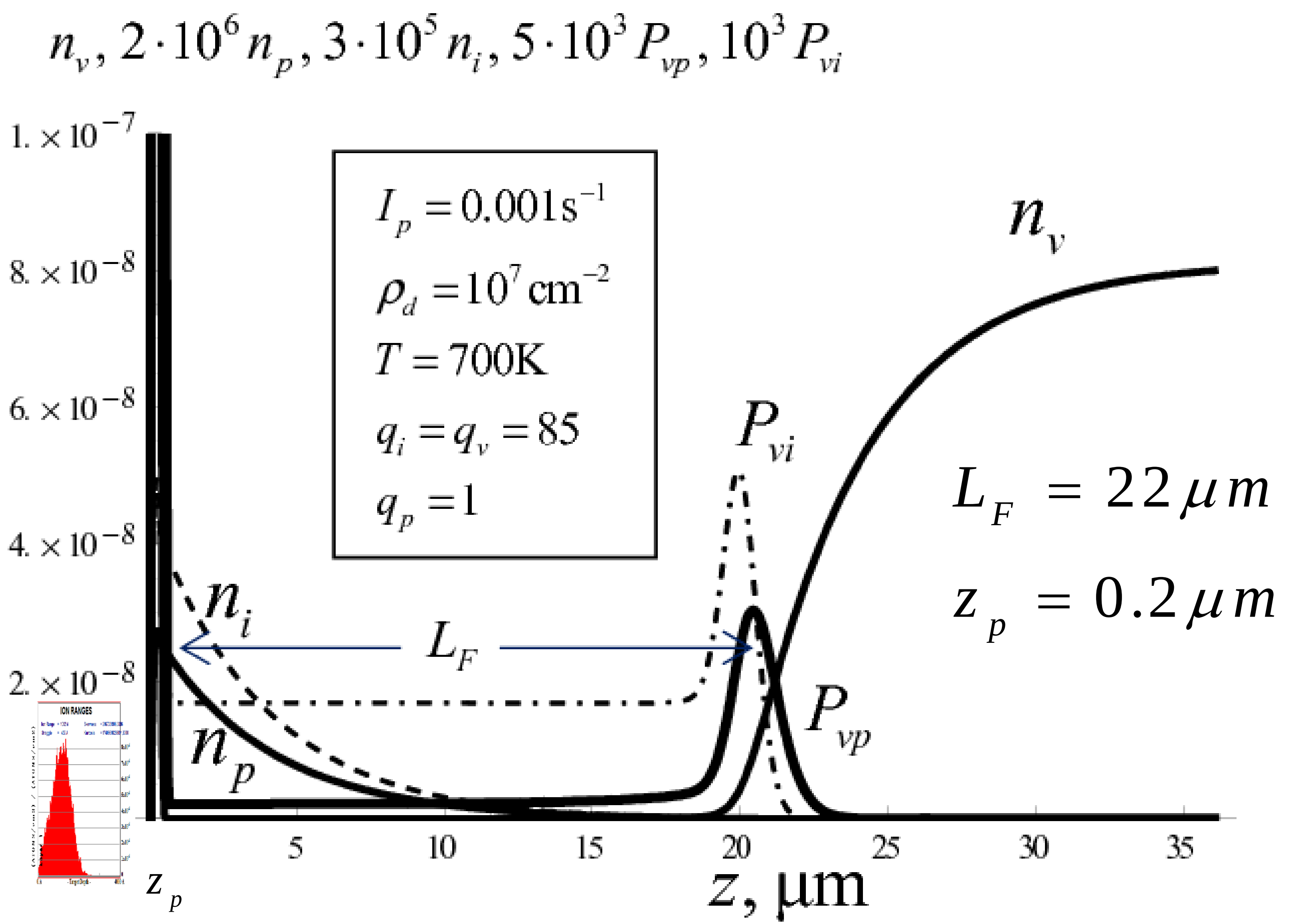

The spatial distributions of the point defect concentrations, recombination rates and complex formation rates

The region beyond the ion range may be divided into two pats. In the first part (close to ion range) there is the excess of atoms in interstitial position, in the other one (far from the ion range) the excess of vacancies takes place. By the analogy with *p-n* junction in semiconductors we suggest the term “ *i-v* junction” (interstitial – vacancy) for the transitional layer between the pats

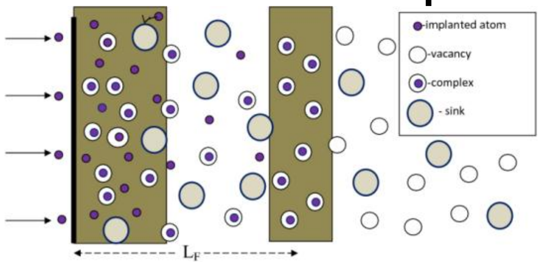

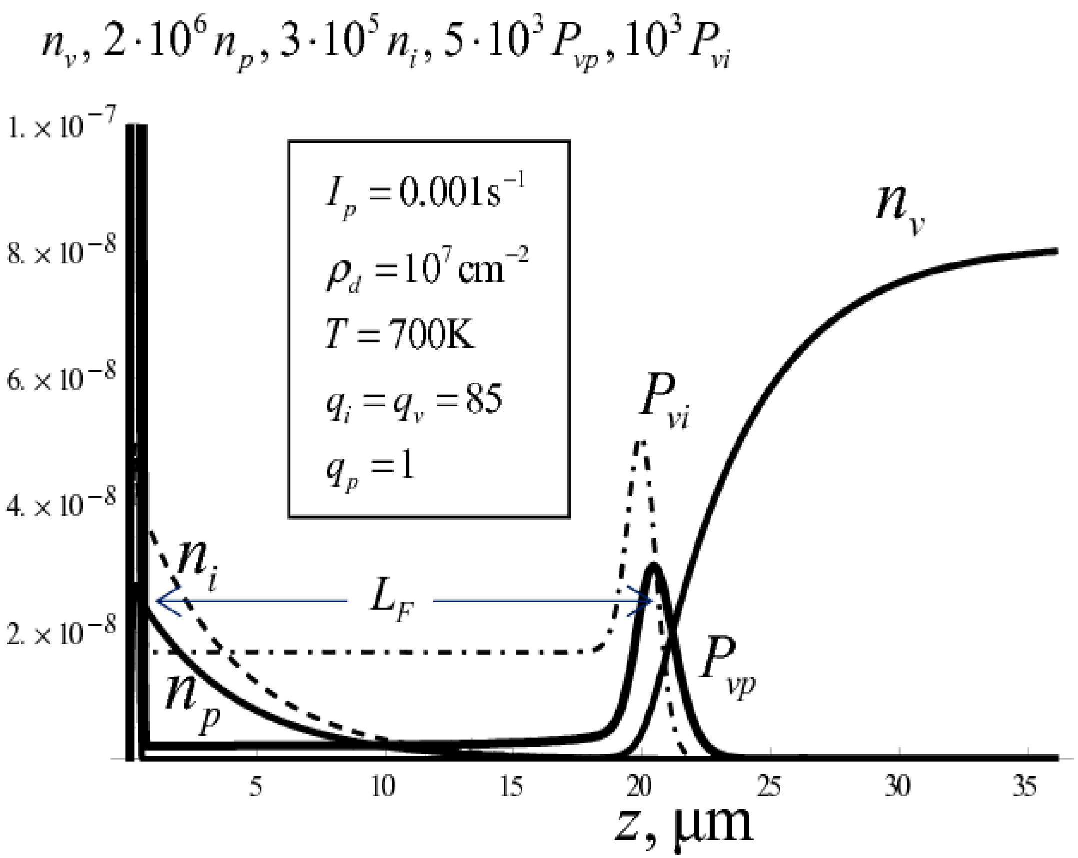

Consequences. Two features.

1) Disappearance of free vacancies in some space (with the size L_F) beyond ion range.

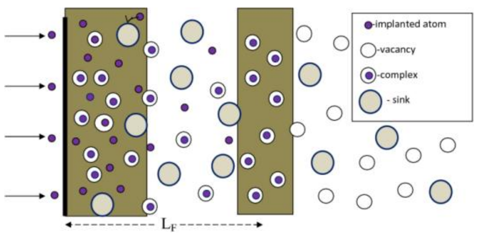

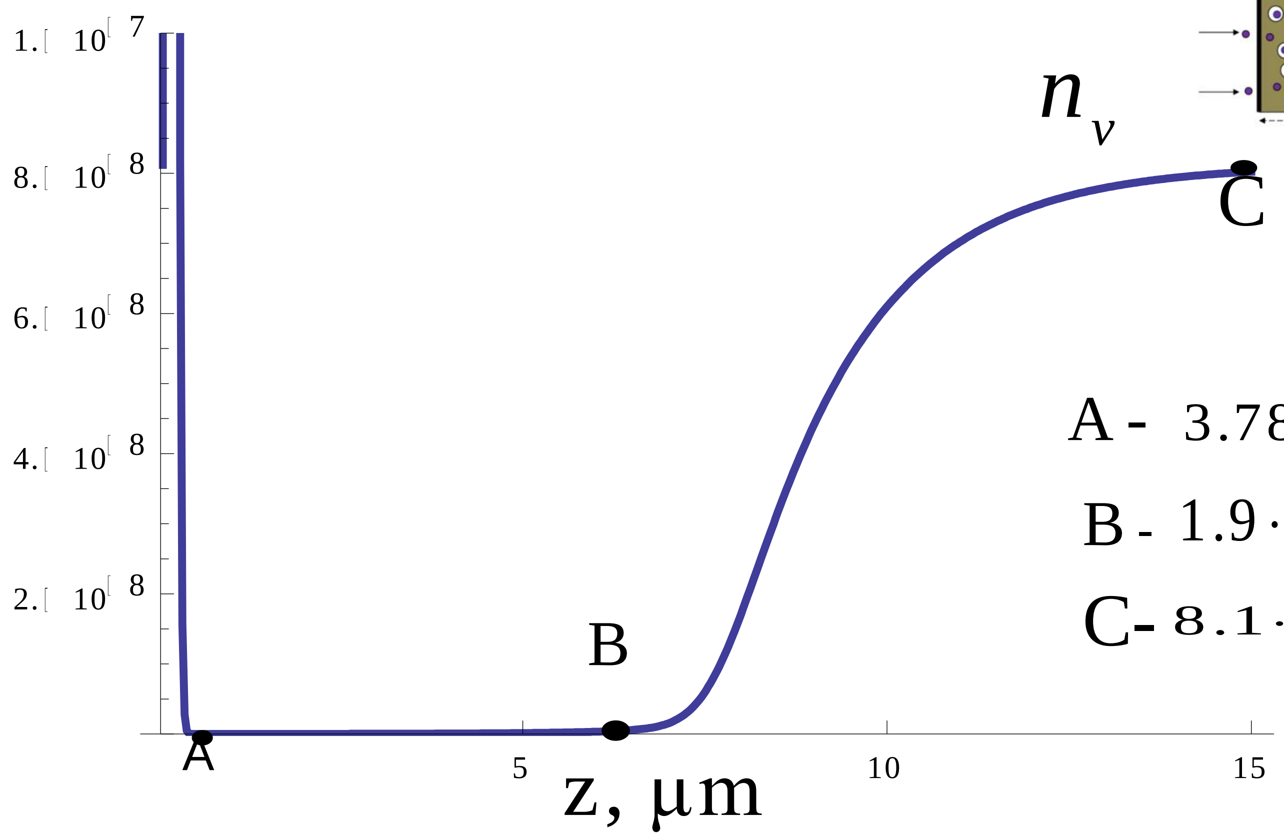

A - $3.78 \cdot 10^{-13}$

B - $1.9 \cdot 10^{-12}$

C- $8.1 \cdot 10^{-8} = n^{th}$

2)The appearance of a spike of the concentration of the implanted atom-vacancy complexes beyond the ion range

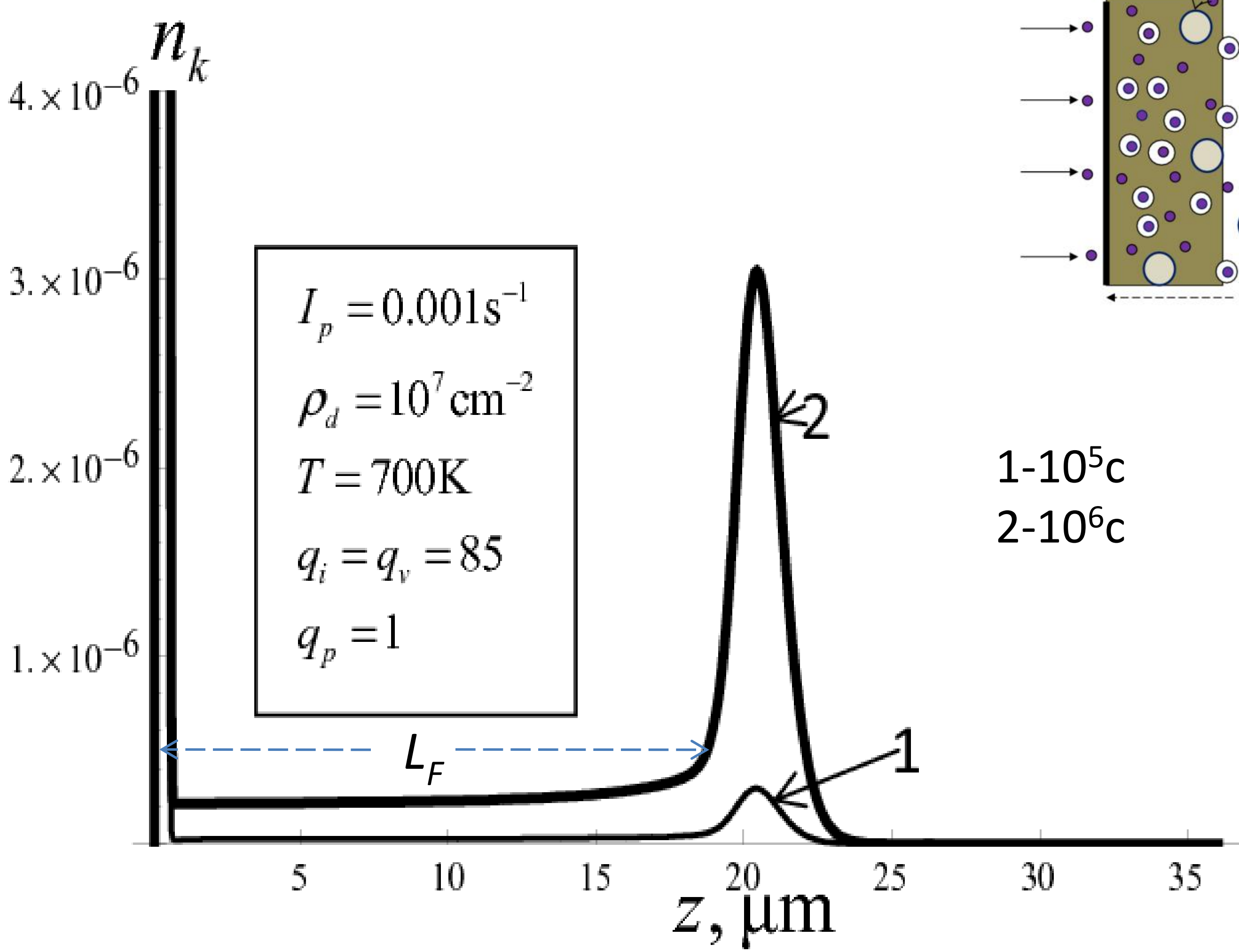

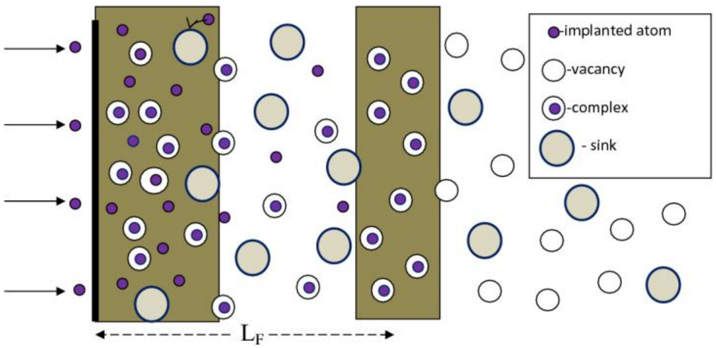

$1\text{-}10^5$c

$2\text{-}10^6$c

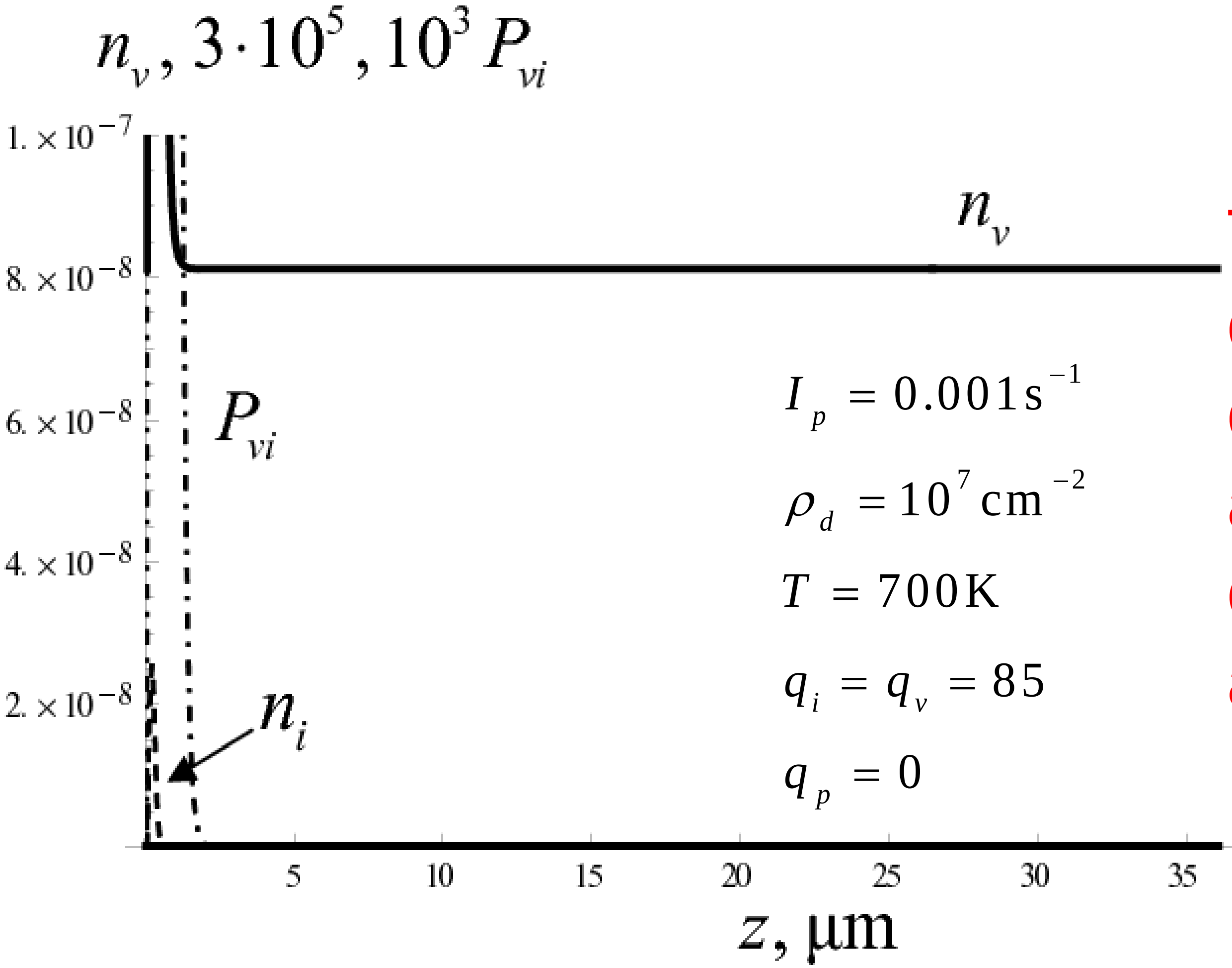

The phenomena of disappearance of free vacancies and appearance of the spike are absent at $q_p = 0$!

The case of the absence of the excess of the number of interstitials (both self-interstitials and implanted atoms) over the number of vacancies created by irradiation ($q_p = 0$).

Effect on physical processes

The change of flux relations of vacancies and interstitial atoms to sinks .

Usually, at point defect creation under irradiation the condition $D_i \ n_i \approx D_v \ n_v$ takes place. As the result, the fluxes of vacancies and interstitials ($\bar{j} = -D \bar{\nabla} n$) are equal.

The presence of a preference in a capture of point defects induces the appearance of a difference between fluxes of interstitials and vacancies. As the result the state of the system changes with time. The existence of the preference is one of reason of swelling of materials. The magnitude of the preference is small $(Z_i - Z_v)/Z \approx 0.1$

But in our case in the region beyond the ion range $n_v \approx 0$ therefore,

$$D_i n_i >> D_v n_v$$

So, though the concentration of point defects in this region is small, the effects generated by them may be important.

As the result

1.The diffusion mechanism of substituent via vacancies disappears.

2. The supersaturation of the region by the interstitials may stimulate the creation of disljcation loops of interstitial type.

3. The supersaturation of the region by the interstitials may stimulate phase transitions.

The threshold behaviour of the effects

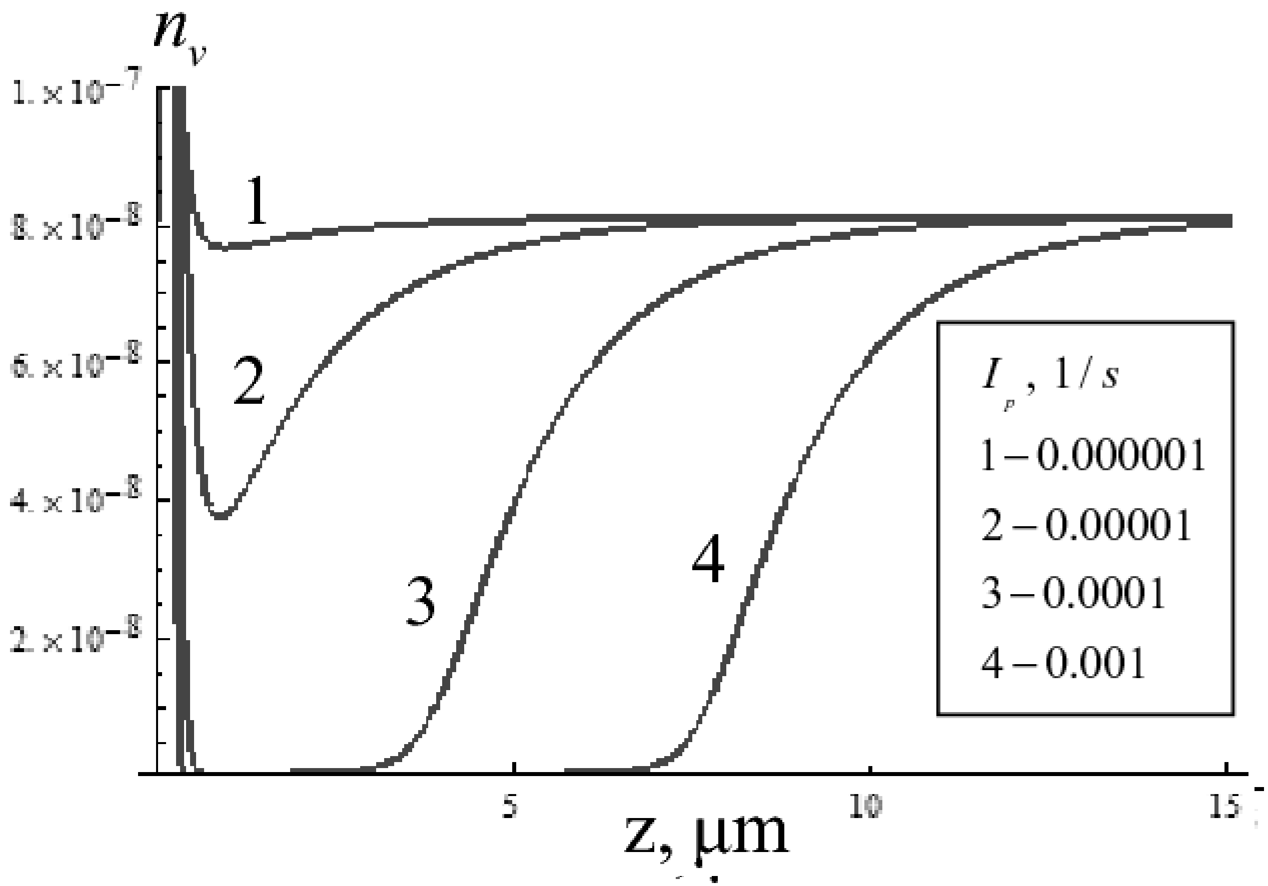

The spatial distributions of the vacancy concentration at different values of the incident flux.

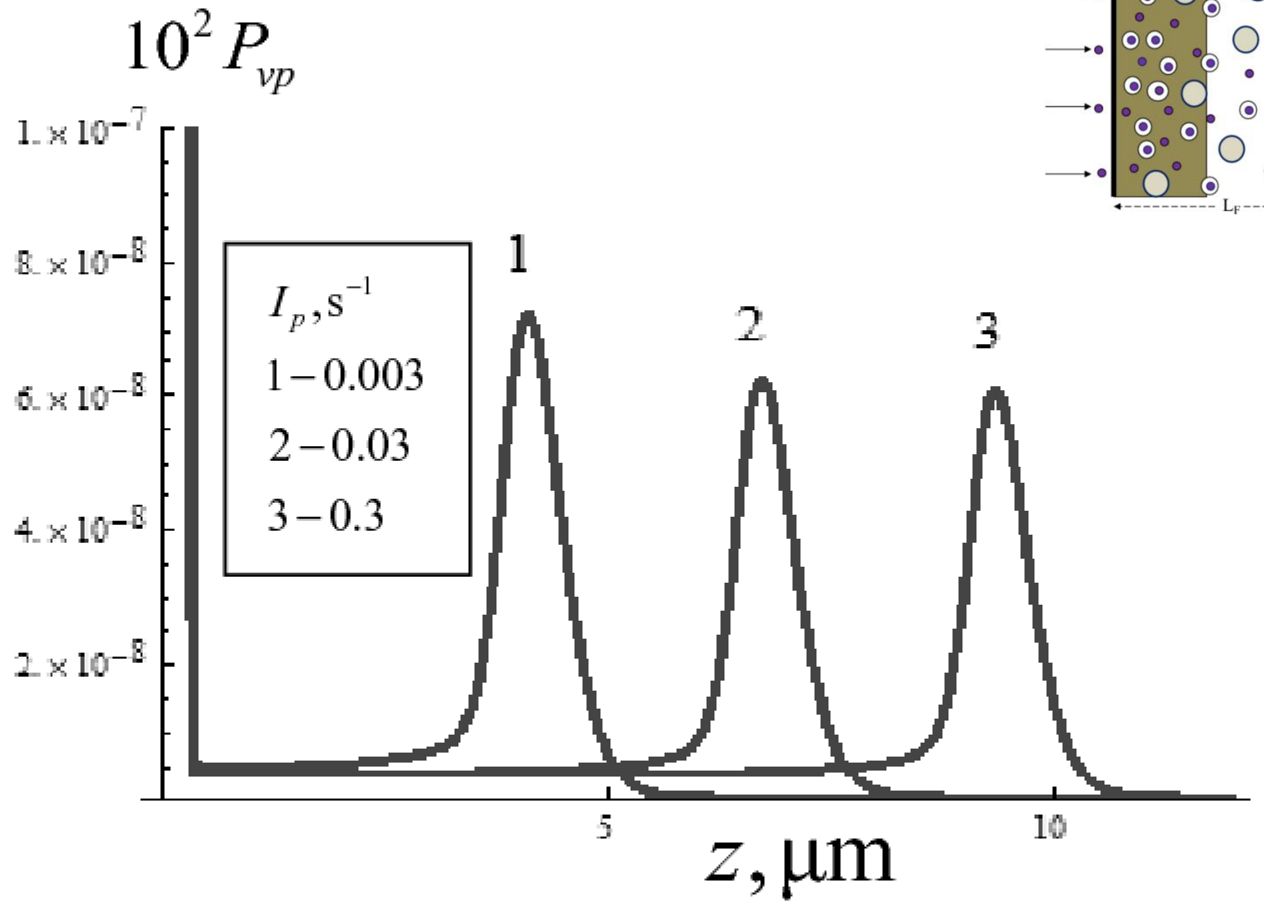

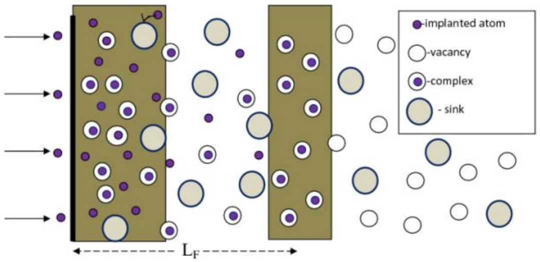

The quasi-stationary spatial distributions of the rate of the binding of the implanted atom with the vacancy for different values of the incident flux.

ρ_d

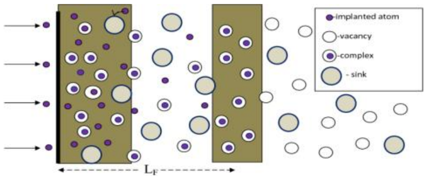

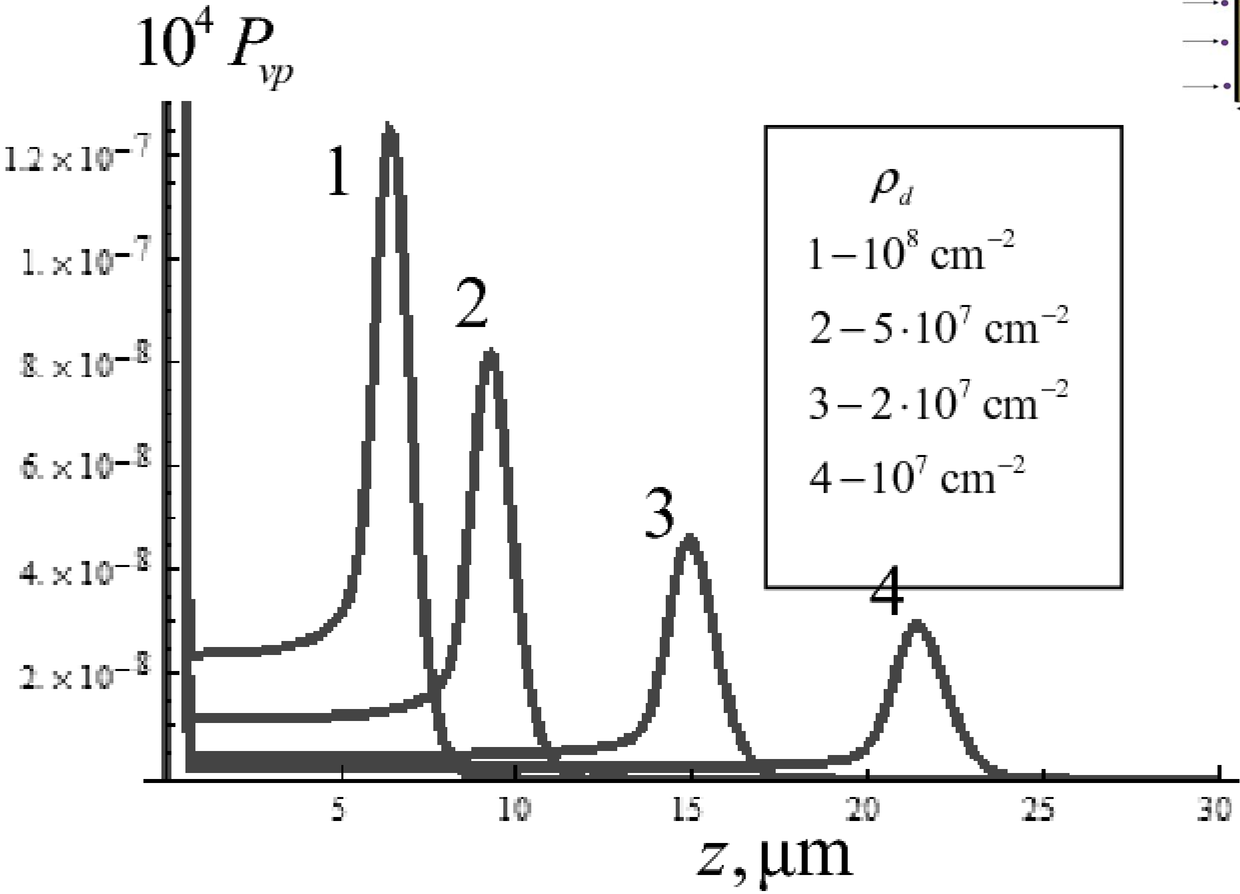

The quasi-stationary spatial distributions of the rate of the binding of the implanted atom with the vacancy for different values of the dislocation density

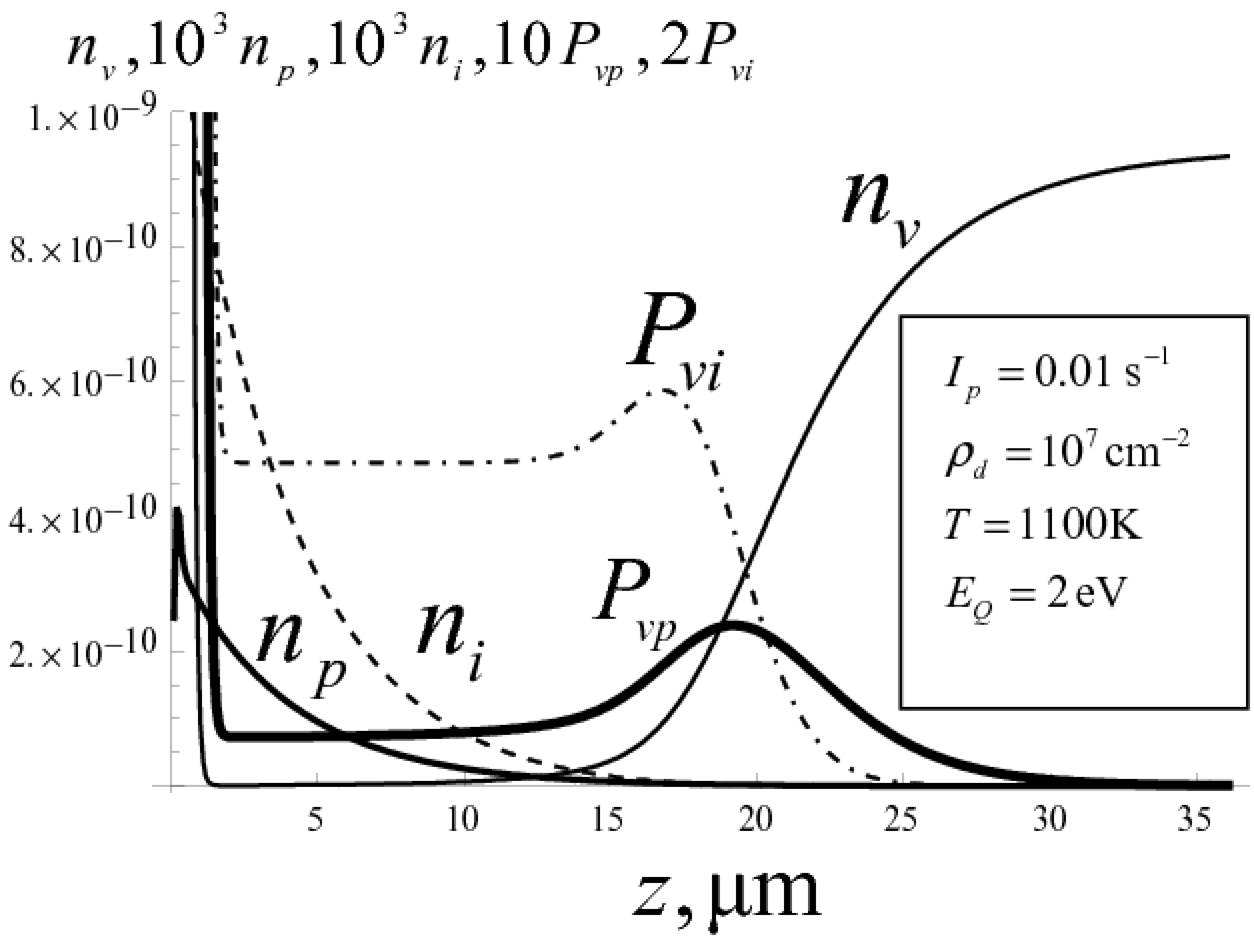

The spatial distribution of the point defect concentration and the defect recombination rate at great value of vacancy formation energy .

The saturable traps

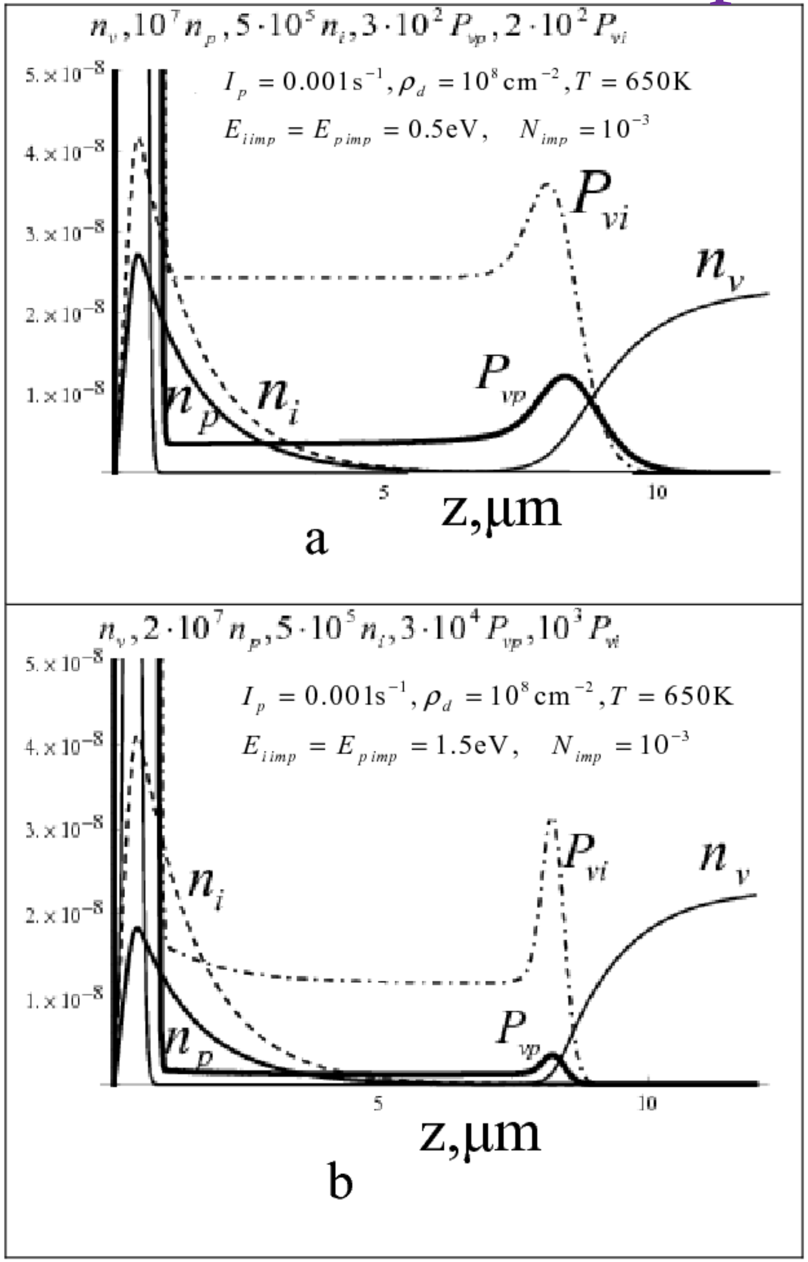

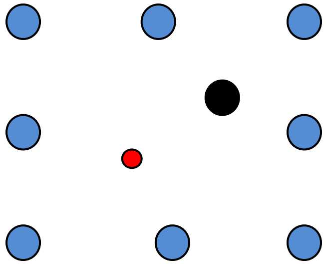

The spatial distributions of the defect density, defect recombination rates and complex-formation rates for the different values of the binding energy of interstitials with sinks

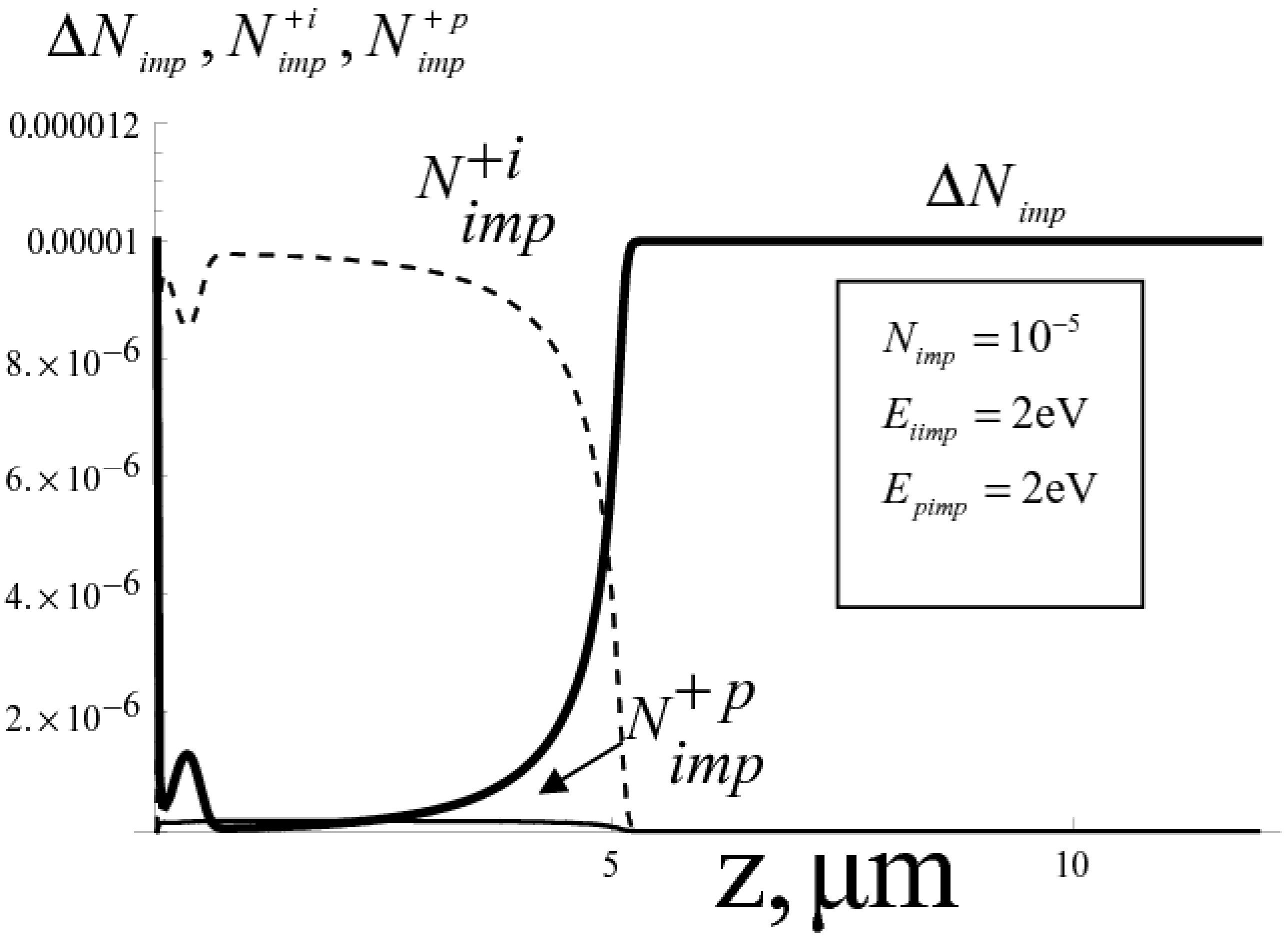

The spatial distributions of the density of the saturable sinks: free sinks (the thick solid line), the sinks with a captured intrinsic interstitial (the thin solid line) and the sink with a captured implanted atom (the dashed line).

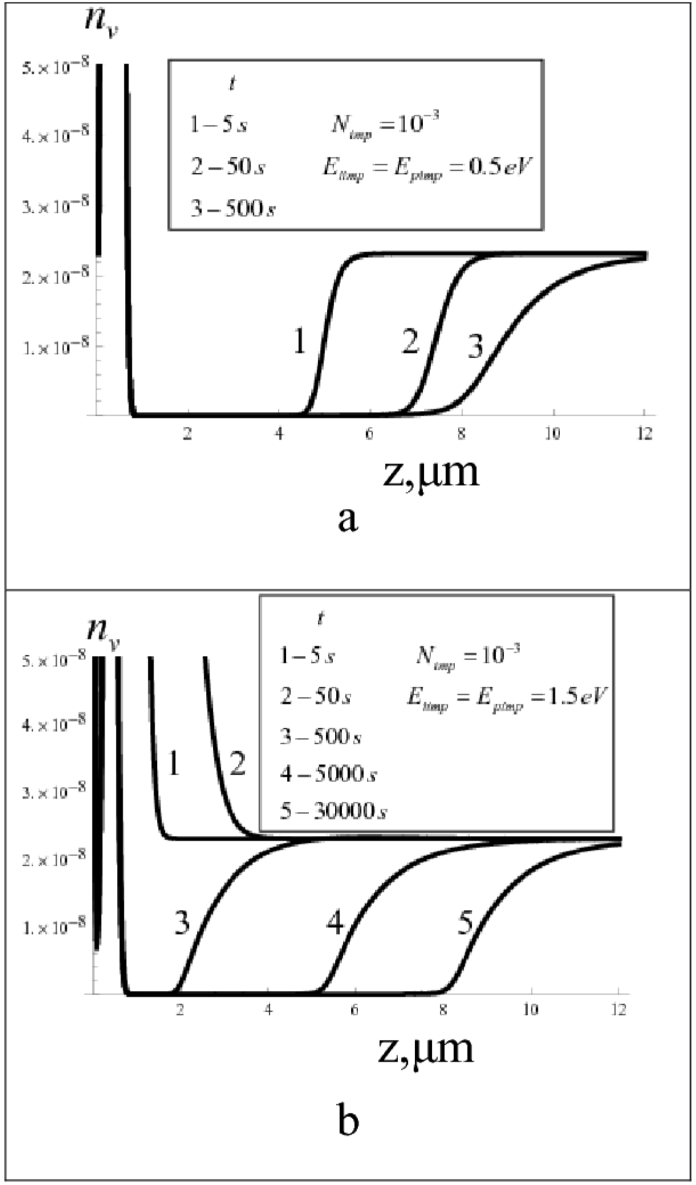

The spatial distributions of the defect density, defect recombination rates and complex-formation rates at different time for the different values of the binding energy of interstitials with sinks:

The deep centers slow down the establishment of the stationary state. With increasing the concentration of saturable centers, the time of the establishment of the stationary state rises.

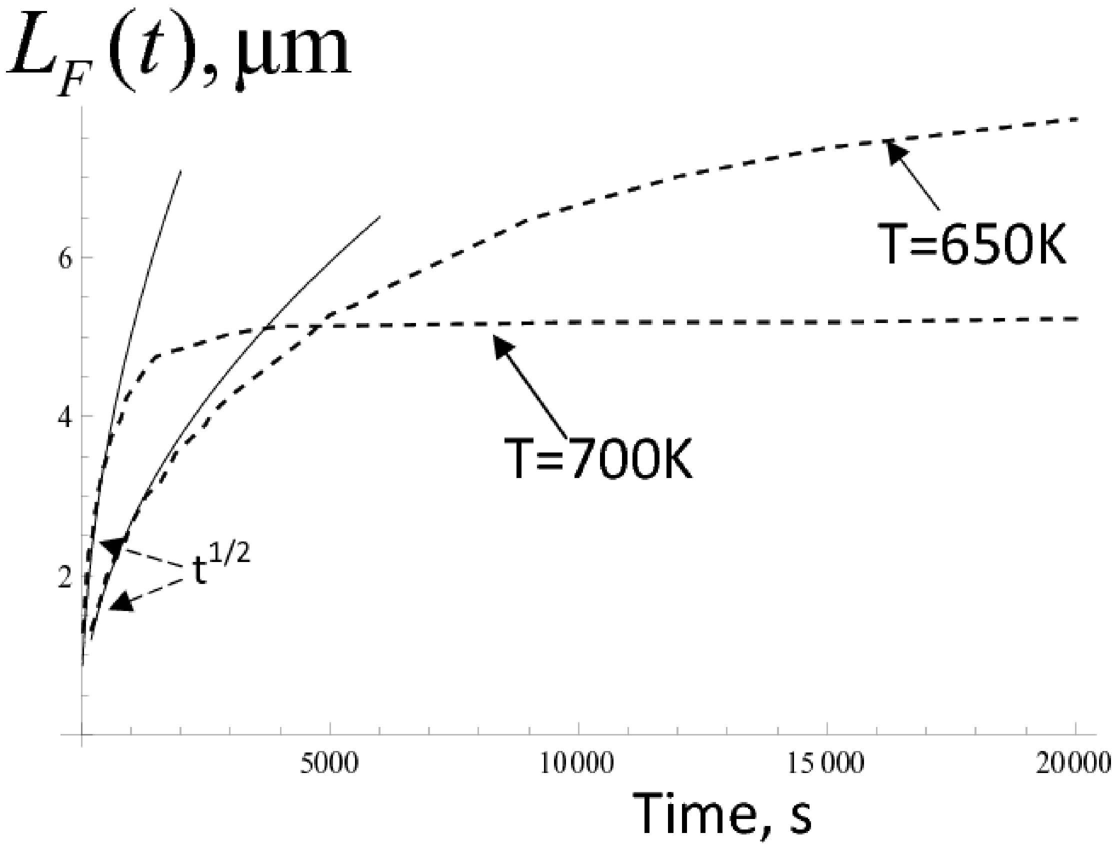

The dependence of the maximum position of the rate of the formation of complexes on time (dashed line) at different temperatures. The time of the establishment of the stationary state shortens with increasing temperature.

He in tungsten

M.J. Baldwin *, R.P. Doerner Journal of Nuclear Materials 404 (2010) 165–173

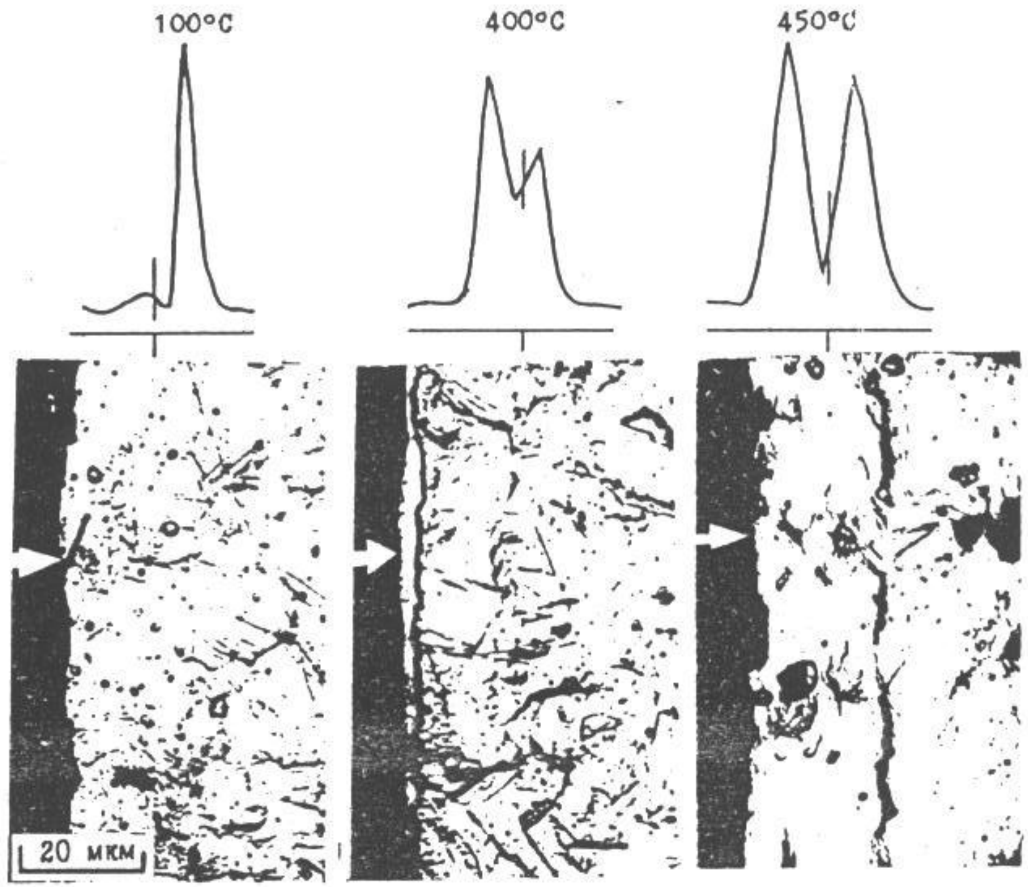

X-ray diffraction lines

"White layers" in the Fe-18Cr-10Ni alloy irradiated (Ar, 50 kev)at different temperatures

Khmelevskaya V.S. at. el.J.Nucl. Mater 1993; Rad. Eff.and Def. in Solids, 1994; Pis'ma in Zh. Tech. Phys. 1996.

The similar effects observed in Fe-Cr и V-Ti-Cr, alloys.

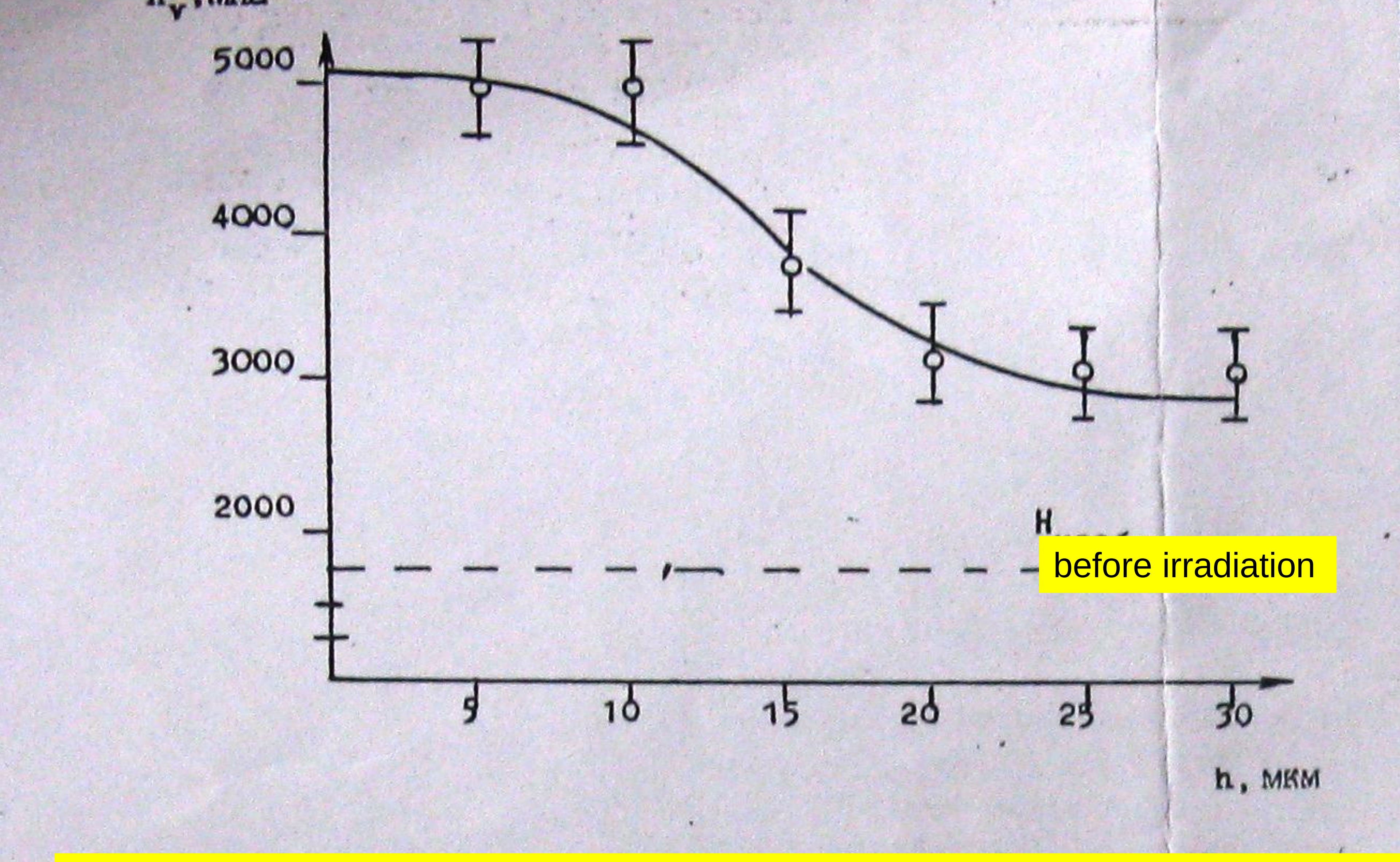

The microhardness dependence in the Fe-18Cr-10Ni alloy on the distance from irradiated surface

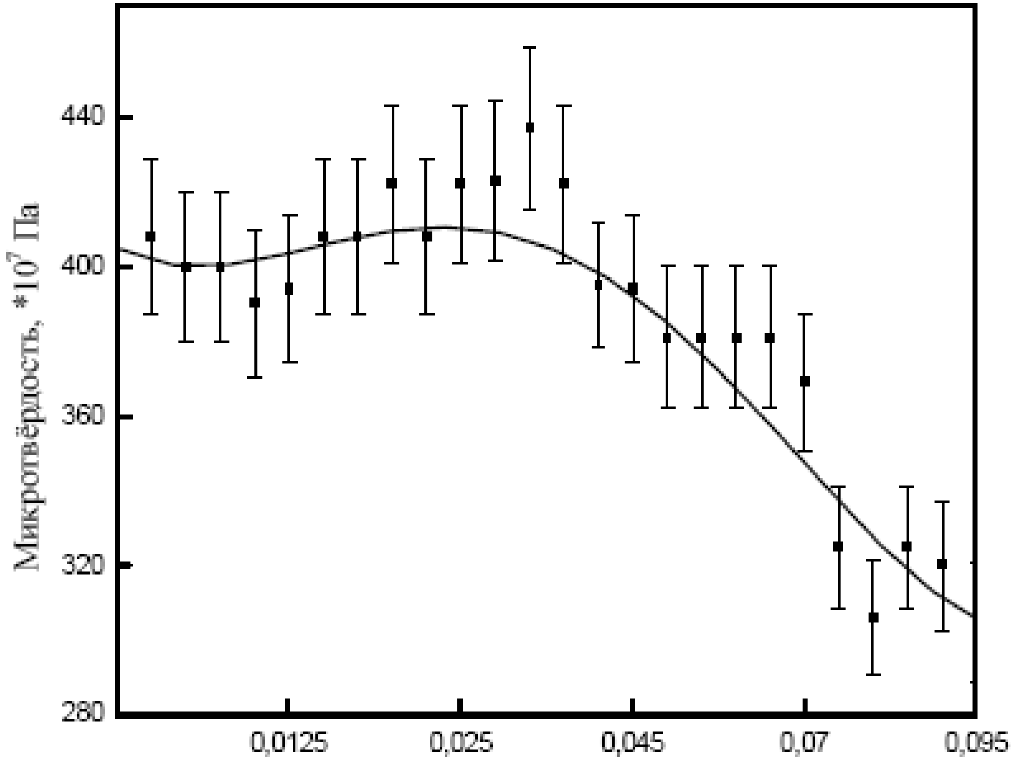

The hardening dependence in the Fe-18Cr-10Ni alloy on the distance from irradiated surface. Ar, 20kev, $1.5 \cdot 10^{18} ion/cm^2, T = 600C$

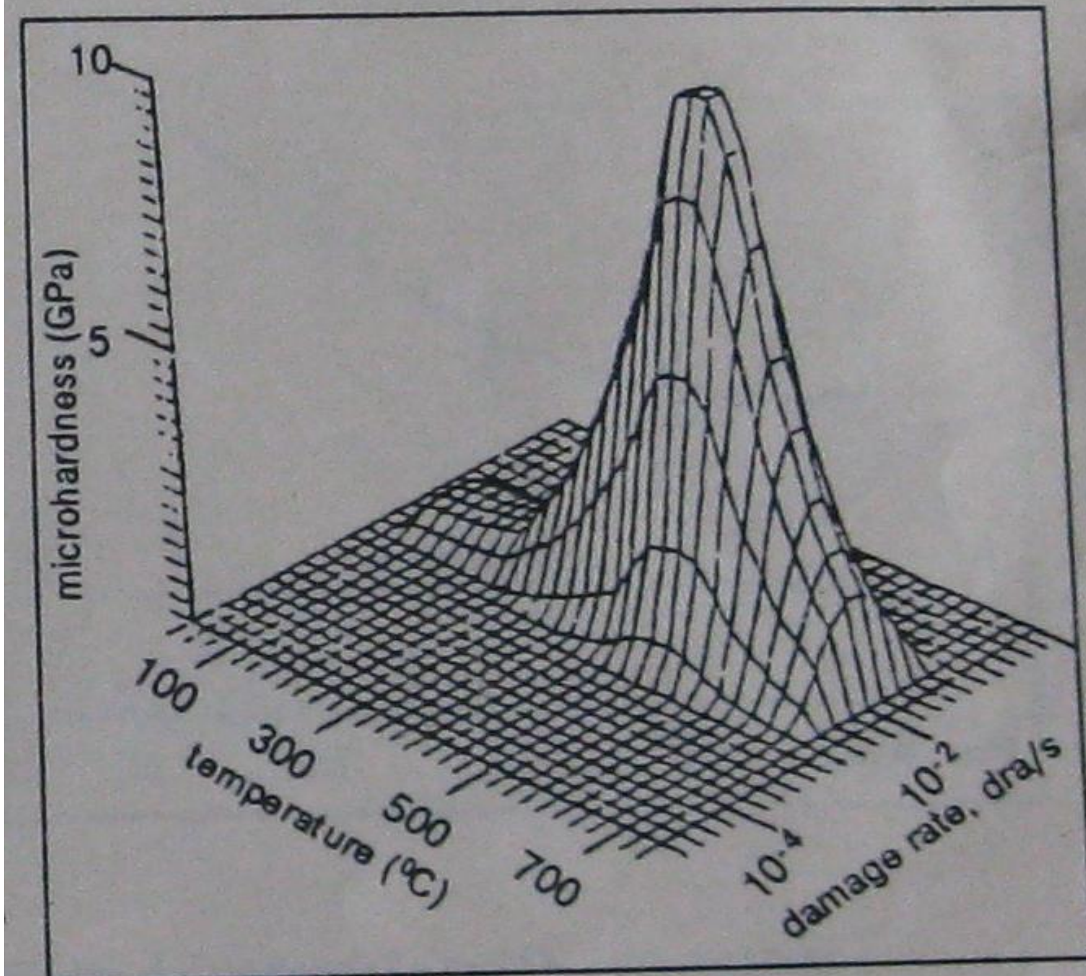

Fig.4. The microhardness dependence of the Fe-18Cr alloy on the irradiation temperature and the flux density (Ar^+, 40 keV, $1,5 \cdot 10^{18}$ ion/cm^2)

V.S. Khmelevskaya, V.G. Malyukin, S.P. Solov’ev. 1996.

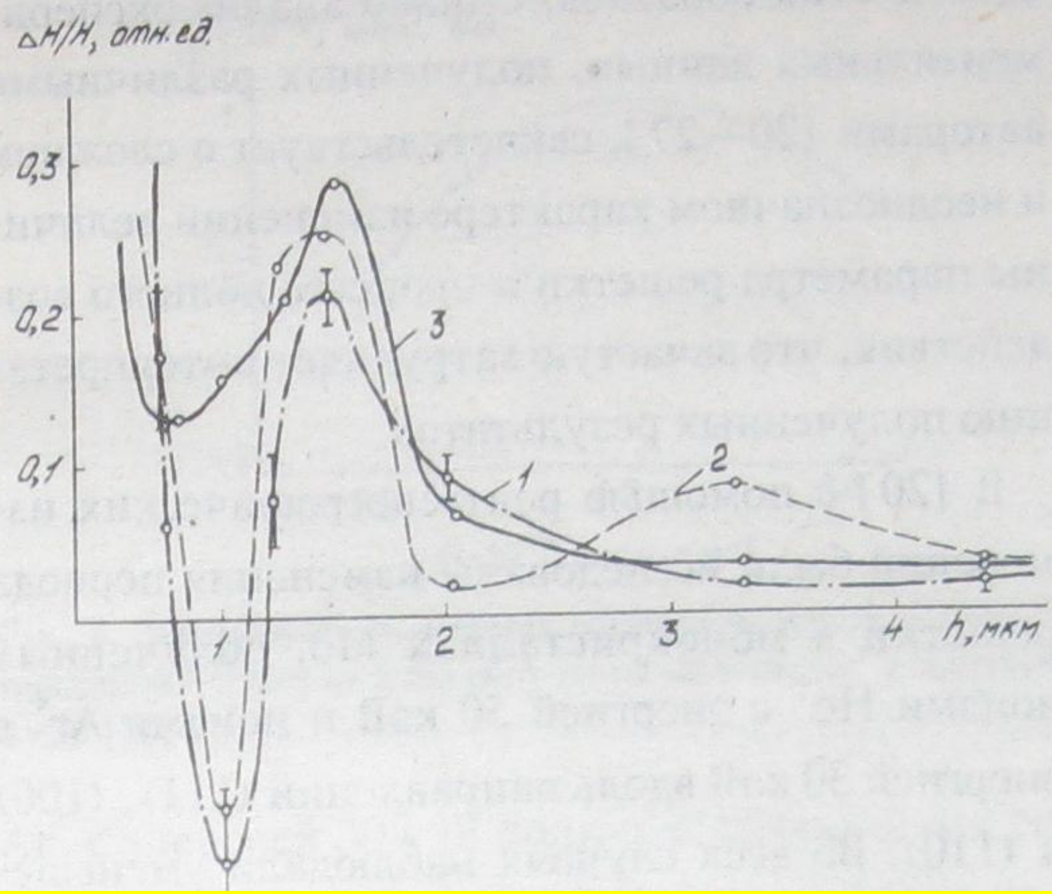

The change of microhardness titanium alloy after irradiation by N ,Ar, N+Ar with energy !20keV

Radzhabov T.D., Basdisaryan A.S. Poverkhnoct', (1986).

M.J. Baldwin *, R.P. Doerner Journal of Nuclear Materials 404 (2010) 165–173

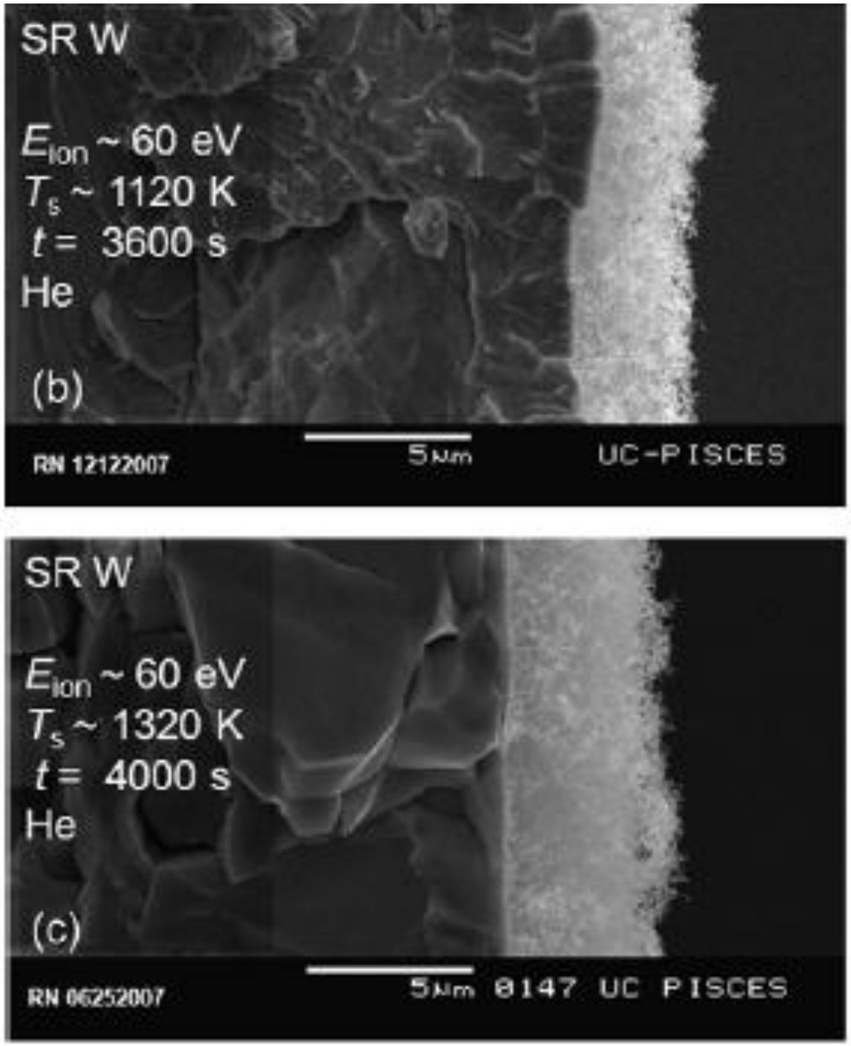

Fig. 2. Cross-sectional SEM micrographs of W targets exposed at (a) 900 K, (b) 1120 K, and (c) 1320 K to pure He plasma for ~1 h.

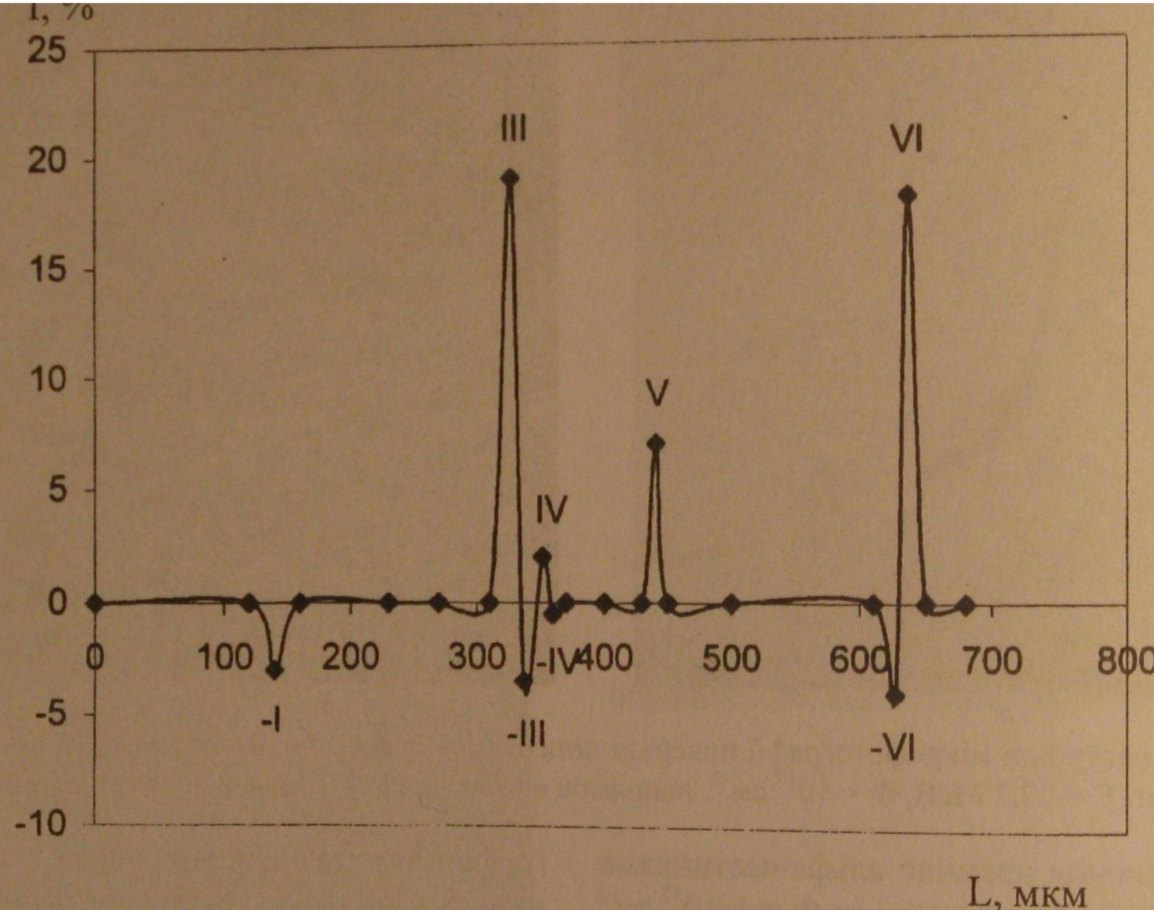

Рис. 4. Фотометрія растрової електронної мікрофотографії (див. рис. 3, *б*) поверхні поперечного перерізу зразка кремнію № 3, опроміненого альфа-частинками, напрямок опромінення по осі абсцис.

A.A Groza, P.G. Litovchenko, M.I. Starchik, V.I. Khivrich, G.G. Shmatko, V.I. Varnina.
Nuclear Physics and Atomic Energy **11**, 66 (2010).

CONCLUSIONS

- The excess of the total number of atoms (self-interstitials and implanted atoms) in the interstitial positions over the number of the vacancies created by irradiation causes a formation of a specific region beyond the projected range, which is strongly depleted of free vacancies and contains complexes consisting of bound implanted atoms and vacancies.
- On the boundary of the region a spatial peak of both the recombination of interstitials with vacancies and creation of complexes arises. The distance of the peak from the ion range may be large, it grows with increasing the incident ion flux and with decreasing the defect concentration in the crystal.
- The frozen of the vacanciesat the temperature much larger than the room temperature should influence physical processes and physical properties of the crystals beyond the ion range.

THANK YOU

Обзоры

- 1. Быков В.Н., Малынкин В.Г., Хмелевская В.С. Эффекты дальнодействия при ионном облучении.// Вопросы атоиной науки и техники. Серия: Физика радиационных повреждений и радиационное материаловедение.- 1989, вып.3(50).-С. 45-52.
- 2. Пивоваров А.Л. Эффект дальнодействия при облучении металлов ионно-плазменными потоками.// Металлофизика и новейшие технологии.// -1994, Т.16, № 12. С -3-17.
- 3. Овчинников В.В. Радиационно-динамические эффекты. Возможности формирования уникальных структурных состояний и свойств конденсированных сред. // УФН. -2008.- Т. 178, вып. 9. - С. 993 -1001.

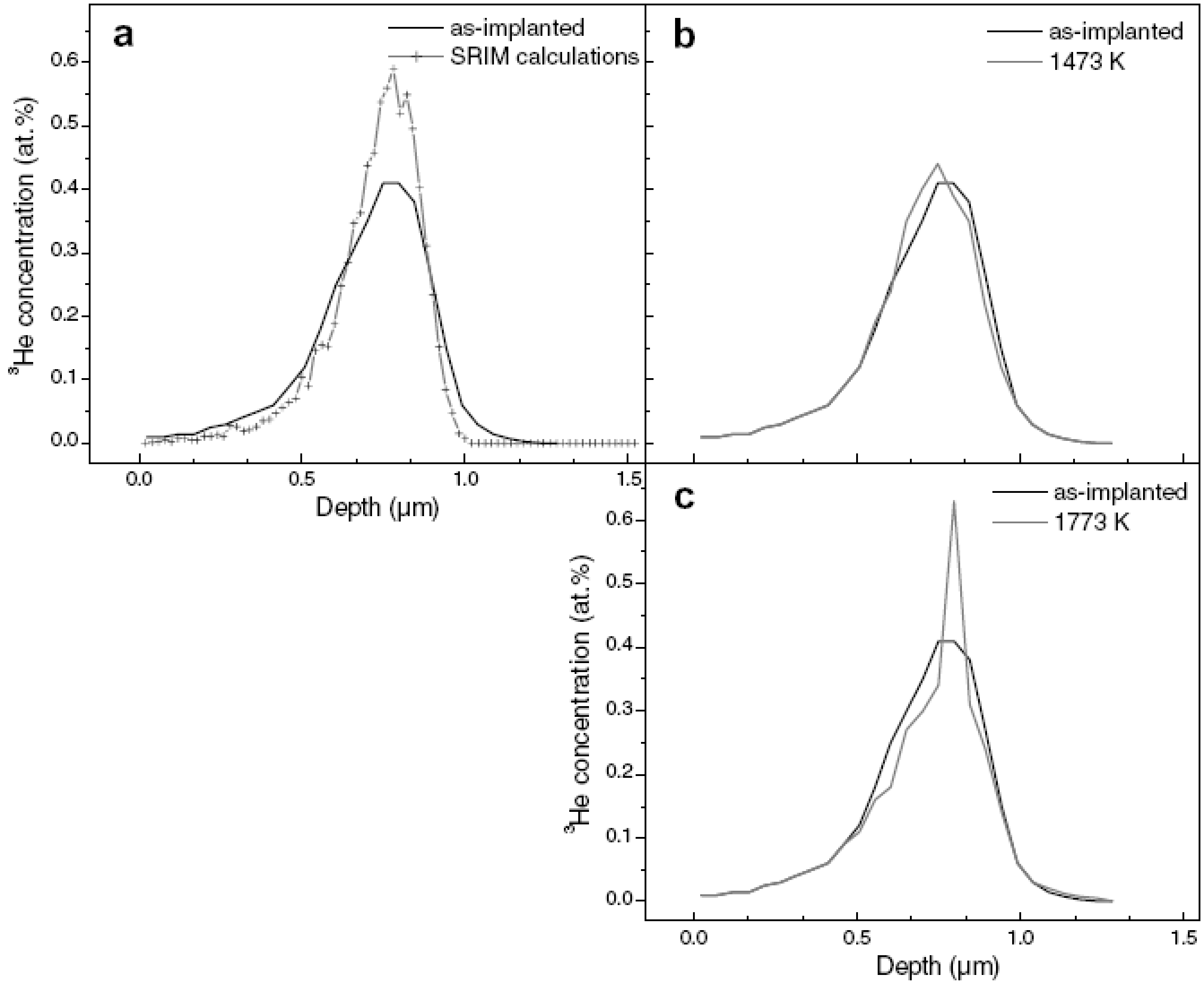

Fig. 3. (a) Theoretical (SRIM calculations) and experimental distributions of 500 keV ^{3}He ions implanted at a 10^{16} cm^{-2} fluence in tungsten at RT; (b) evolution of the experimental implantation profile after a thermal annealing at 1473 K during 70 min under vacuum and (c) after a thermal annealing at 1773 K during 1 h under $Ar–H_2$ atmosphere.